

An Empirical Correlation Between Glass Transition Temperatures and Structural Parameters for Polymers with Linear and Branched Alkyl Substituents

HANG GAO AND JULIE P. HARMON

Department of Chemistry, University of South Florida, 4202 E. Fowler Ave., CHE 305, Tampa, FL 33620

Received 7 August 1996; accepted 19 September 1996

ABSTRACT: A new quantitative model is proposed to correlate glass transition temperatures with bond radii-based structural parameters for poly(*p*-alkyl styrenes), polyolefins, poly(alkyl methacrylates), and poly(alkyl acrylates). The model provides a consistent prediction of the glass transition temperatures for both the linear and highly branched polymers up to the entanglement offset points for long side groups. Polymers with highly branched side chains, such as *t*-butyl and *t*-pentyl groups that contain quaternary C groups, are predicted to have much higher glass transition temperatures, followed by the methylated, the unsubstituted, and the linearly alkylated polymers. The predictions are confirmed by the experimental results from the authors' research and literature. The current model also allows the extraction of the contribution of hydrogen bonding to glass transition temperatures in polymethacrylates and polyacrylates by comparing differences between the modeled hydrogen-bonding free values with the experimental data. © 1997 John Wiley & Sons, Inc. *J Appl Polym Sci* **64**: 507–517, 1997

Key words: glass transition temperature; structural parameter; polystyrenes; polyolefins; polyacrylics

INTRODUCTION

The importance of the measurement and the understanding of the effects of structure on the glass transition temperatures of amorphous materials cannot be overestimated. There is a large amount of practical and theoretical work that has been carried out in an attempt to correlate the glass transition temperatures of polymers to structural, thermodynamic, statistical and quantum mechanical properties.^{1–5} Cohesive energy was one of the properties utilized in early correlations.^{6–8} Molar volume of the polymer segment units was incorporated in Marcincin's calculation.⁷ By his calculation, polymers with larger molar volumes should have proportionally higher glass transition

temperatures. However, many discrepancies were found.^{9,10} The steric hindrance factor, σ , of the polymer chains was taken into consideration by Vincent,¹¹ Aharoni,¹² Boyer and Miller,^{13,14} and He.¹⁵ They showed that the steric hindrance affects the readiness of molecular movement of the polymer chains and thus the glass transition temperature of polymers. The steric hindrance factor was further correlated with volume elements, such as the crystalline unit cell volume¹⁶ and the cross-sectional area of polymer chains.¹⁵ Chee¹⁷ further noted a break point in the dependence of glass transition temperature on the "intensive variable B " (related to solubility parameters). Chee found that when $B \leq 380$ J/mL, the glass transition temperature is a function of both the chain flexibility and intermolecular interactions. When $B > 380$ J/mL, T_g only depends on intermolecular interactions. On the other hand, the estimation of glass transition temperatures by molec-

Correspondence to: Julie P. Harmon.

© 1997 John Wiley & Sons, Inc. CCC 0021-8995/97/030507-11

ular modeling has been carried out by Hopfinger, Koehler, Pearlstein and Tripathy.¹⁸ In their study, the conformational entropy and the mass moment of the polymer were calculated in terms of torsional angles. The bond lengths and sizes of components were not taken into account. Molecular dynamics simulations have recently been used to estimate glass transition temperatures for polymers such as amorphous *cis*-poly(1,3-butadiene), polyisobutylene, atactic polypropylene and atactic polystyrene.¹⁹ Group contribution methods, although empirical methods, have achieved great practical applications,^{1-3,9} after systematically being introduced by van Krevelen and Hof-tyzer.⁹ They presented a general formula,

$$T_g = \frac{Y_g}{M} = \frac{\sum Y_{gi}}{M} \quad (1)$$

where Y_g and Y_{gi} are the molar glass transition functions of overall and individual group contributions respectively. M is the molar mass of the repeat unit. Wiff, Altieri and Goldfarb²⁰ further developed a database, based on group contribution calculations and chemical structural parameters from about 200 polymers. The most recent compilation of group contribution tables is found in reference 3. Bicerano² applied the connectivity index method to polymers. This method is based on a topological interpretation of structure-property correlations, where the structures of molecules are reduced to vertices (atoms) and edges (bonds) which are assigned with different indices, depending on the electronic and structural environment.

For polymers without complex and lengthy pendant group modifications, most of the above-mentioned methods yield reasonable predictions. However, when there are long or highly branched alkyl substituents, the prediction of the glass transition of such polymers tends to deviate significantly. This has been noted for poly(*p*-alkyl styrenes) studied by the authors and several others. Experimental and calculated values of T_g are plotted in Figure 1 and compared in Table I for the poly(*p*-alkyl styrene) series and also the poly-(alkyl methacrylate) series. The experimental value of T_g for polystyrene is about 370 K; however the calculated value from the group contribution method is only 200 K, showing a difference of 170 K. When there is a highly branched alkyl group such as the *t*-butyl group, the T_g is not predicted adequately by group contribution methods

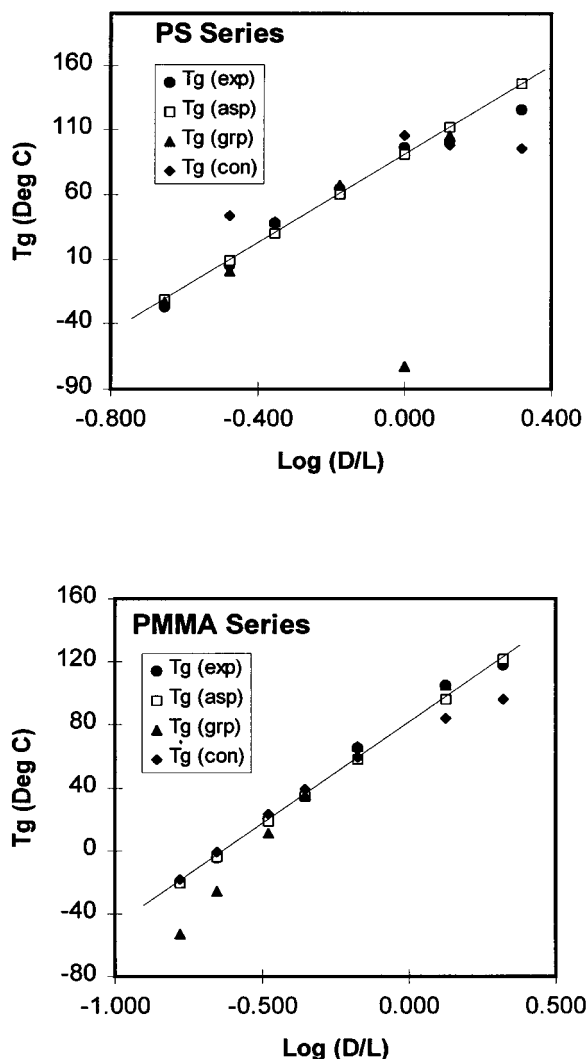


Figure 1 Plot of experimental and calculated values from different computational methods: exp = experimental;^{2,21,24} asp = structural parameter; grp = group contribution;⁹ and con = connectivity index.² D/L is the ratio of the cross-section dimension to the length of the pendant group. See text for calculation. The straight line connects all the calculated values from the asp method, which correspond closest to the experimental data.

since no general group contribution value is available.⁹ The connectivity index method predicts that poly(*p*-*t*-butyl styrene) has the lowest T_g with a higher T_g for poly(*p*-methyl styrene) and polystyrene having the highest T_g (Table I). Experimental data for the three commercially available polymers prove to follow the reverse order. The authors developed a calculation method, the structural parameter method, that uniformly predicts the glass transition temperatures for poly-

Table I Comparison of Experimental and Calculated T_g s (Deg C) for Series of PaS and PaMA

Poly(alkyl styrene)							
-Alkyl	T_g (exp) ^a	T_g (asp) ^b	Dev.	T_g (grp) ^c	Dev.	T_g (con) ^d	Dev.
H	97	88	9	-73	170	106	9
methyl	101	101	0	106	5	98	3
ethyl	65	61	4	67	2		
<i>n</i> -propyl	38	33	5	39	1		
<i>n</i> -butyl	5	11	6	1	4	44	39
<i>t</i> -butyl	126	135	9			96	30
<i>n</i> -hexyl	-27	-21	6	-23	4		
Average dev.			6		31		20
Max dev.			9		170		39
Min dev.			0		1		3
Poly(alkyl methacrylate)							
-Alkyl	T_g (exp) ^a	T_g (asp) ^b	Dev.	T_g (grp) ^c	Dev.	T_g (con) ^d	Dev.
methyl	105	97	8	105	0	84	21
ethyl	65	62	3	66	1	59	6
<i>n</i> -propyl	34	38	4	35	1	39	5
<i>n</i> -butyl	20	19	1	11	9	23	3
<i>t</i> -butyl	118	128	10			96	22
<i>n</i> -hexyl	-5	-9	4	-26	21	-1	4
<i>n</i> -octyl	-20	-30	10	-53	33	-18	2
Average dev.			6		11		9
Max dev.			10		33		22
Min. dev.			1		0		2

^a exp = experimental method.^{2,21,24}

^b asp = structural parameter method developed by the authors.

^c grp = group contribution method.⁹

^d con = connectivity index method.²

mers such as poly(alkyl styrenes), PaS, studied intensively in our research,²¹⁻²³ as well as poly(alkyl methacrylates), PaMA, poly(alkyl acrylates), PaA, and polyolefins, PO, in which long linear and highly branched substituents are often encountered. Figure 2 shows the basic structures of these polymers.

A STRUCTURAL PARAMETER MODEL FOR LINEAR AND SYMMETRICALLY BRANCHED ALKYLATED POLYMERS

Although the effects of alkylation and alkyl branching in polymers have not been quantitatively and systematically calculated, they have been noted by many researchers.^{24,25} Stevens²⁵ summarized that linearly increasing the length of pendant groups results in a decrease in glass transition temperature. This decrease continues until the entanglement of pendant groups is offset

and there is a recoil in glass transition temperature with an increase in side group length. The decrease of T_g is widely believed to be a plasticizing effect of the side chains that act similar to small molecular weight additives.^{25,26} For poly(*p*-alkyl styrenes) this takes place when the number of carbon, *n*, reaches 10; for poly(alkyl methacrylates), *n* = 18; for polyolefins, *n* = 6; and for poly(alkyl acrylates), *n* = 7.^{25,26} On the other hand, the increase in glass transition temperature can be significant when there is branching in the alkyl groups.

The current authors' study of a para-alkylated polystyrene series including polystyrene, poly(*p*-methyl styrene), poly(*p*-ethyl styrene), poly(*p*-*n*-propyl styrene) and poly(*p*-*t*-butyl styrene) by differential scanning calorimetry, dielectric analysis, and dynamic mechanical analysis²¹⁻²³ agrees favorably with published experimental results.^{2,9,24,25,27} A unified model to account for the glass transition temperature effect due to alkyl-

ation via both linear lengthening and branching in polymers is proposed here. As shown in Figure 1 and Table I, this method correctly predicts that poly(*p*-*t*-butyl styrene) has the highest glass transition temperature followed by poly(*p*-methyl styrene) and polystyrene, etc. The current model emphasizes the quantitative correlation between the glass transition temperatures and the geometry of the alkyl groups for the side groups, up to the plasticizing offset point. Past this point, the calculation becomes more complex due to entanglements in the side groups and possibly with the main chains; this situation is not dealt with here. The calculation is easily carried out without sophisticated computer hardware and software. It only involves the knowledge of bond radii of carbon, oxygen, and hydrogen. Figure 3 shows this model schematically with polystyrene as an example. The following summarizes the key assumptions used in this structural parameter model.

1. The repeat unit of the polymer without its alkyl pendant group is considered a basic unit; thus, in Figure 2, (I) is the basic unit for the polystyrene series, (II) for the polymethacrylate series, (III) for the polyacrylate series, and (IV) for the polyolefin series. All basic units have one open bond that allows for alkyl substitution. By adding $-\text{H}$, $-\text{CH}_3$, $-\text{C}_2\text{H}_5$, \dots , alkylated series are obtained.
2. The alkyl group is composed of one or more cylindrical sections, each of which is repre-

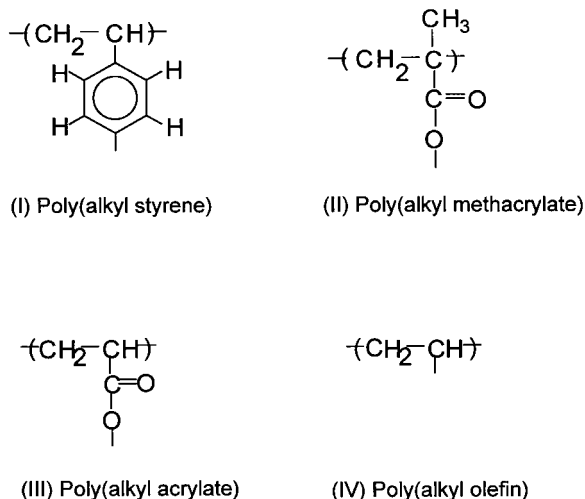


Figure 2 Structures of the basic units for four polymer series studied; poly(alkyl styrene), poly(alkyl methacrylate), poly(alkyl acrylate), and polyolefin.

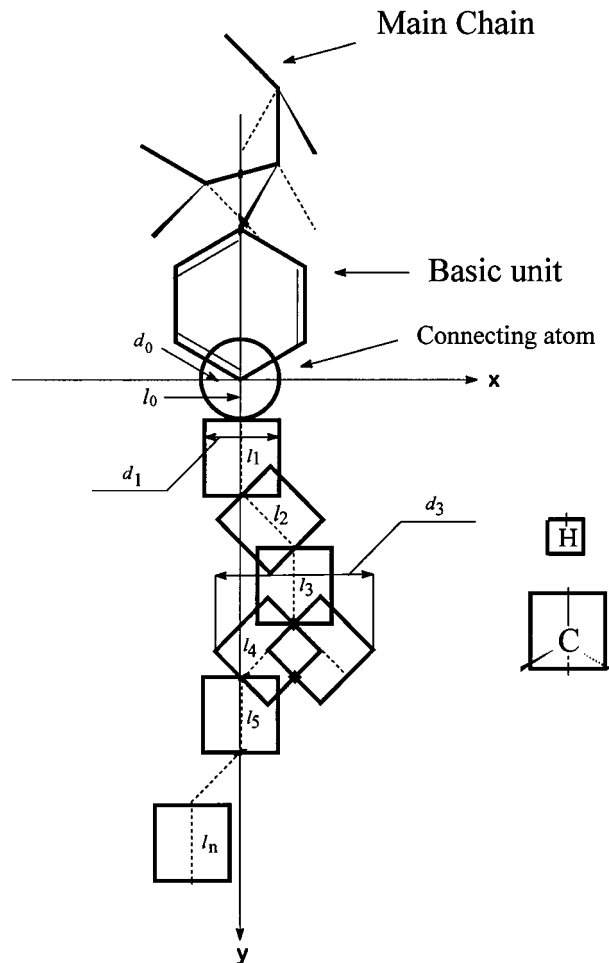


Figure 3 Structural parameter model of calculation. The basic structure is poly(alkyl styrene), as an example. See text for detailed explanation.

sented by one carbon and covalent-bonded hydrogens or other carbons, like the boxes shown in Figure 3. In the case of no alkyl substitution, H is the terminal atom and has a cubic box of the dimensions of a hydrogen atom. All sections can rotate along the bonding axes freely to reach the maximum radii.

3. The origin of the coordinate is set in the center of the last connecting atom in the basic unit. For PaS and PO, carbon is the connecting atom and for PaMA and PaA, oxygen is the connecting atom. The y axis is defined as the line passing through the bond of the connecting atom and the first carbon or hydrogen in the substituent group and pointing away from the basic unit. The x axis is perpendicular to the y axis and is in the plane of the basic unit.

The effective diameter of the alkyl side group is defined as the average of the diameters of all sections,

$$D = \frac{\sum_{i=0}^n d_i}{n + 1} \quad (2d_0 > d_i) \quad (2)$$

and,

$$D = \frac{\sum_{i=1}^n d_i}{n} \quad (2d_0 \leq d_i) \quad (3)$$

d_0 is the diameter of the connecting atom in the basic unit, and $d_1 \cdots d_n$ are the diameters of all the sections in the side group. It is noted that the comparison of the diameters of the connecting atom d_0 and the connected sections d_i ($i = 1 \cdots n$) is necessary since, when branching occurs ($d_i > 2d_0$), especially in the first few sections close to the basic unit as in the case of *t*-butyl and *t*-pentyl sections, the connecting atom is basically contained in the umbrella formed by this section. Thus, it should be excluded from the averaging process from equation (2)—see the 3-D modeling of polymethylstyrene and poly(*p-t*-butyl styrene) Figure A.1 and Figure A.3 in Appendix A. This situation is reflected in equation (2). The effective length of the alkyl group is the scalar sum of lengths of all the sections, corresponding to the above two cases,

$$L = \sum_{i=0}^n l_i \quad (2d_0 > d_i), \quad (4)$$

and,

$$L = \sum_{i=1}^n l_i \quad (2d_0 \leq d_i) \quad (5)$$

l_0 is the radius of the connecting atom and $l_1 \cdots l_n$ are the lengths of all the sections in the side group.

4. Before the pendant group reaches its plasticizing offset length, the glass transition temperature of a polymer thus formed decreases with the increase in the length of the pendant group, L , but increases with the increase in cross-section dimension of

the pendant group, D . Glass transition temperature, T_g , is linearly proportional to the logarithm of D/L .

$$T_g = T_{g0} + k \log (D/L) \quad (6)$$

where T_{g0} and k are temperature constants dependent on specific polymer series.

The above assumption idealizes the alkyl groups and their immediate environment, which is believed reasonable due to the electronic intermolecular interaction which is very limited as a result of the non-polar nature of the alkyl groups. The low rotational energy ($2 \sim 4.2$ kcal/mol²⁶) of C—C bond within the alkyl group can be basically ignored. This makes the calculation of the properties much simpler since no torsional angles need to be included. The calculation for d and l values of the basic sections, i.e., the nonsubstituted hydrogen and primary, secondary, tertiary and quaternary carbons via this model, is outlined in Appendix A.

RESULTS AND DISCUSSION

Table I shows the predicted glass transition temperatures for the polystyrene and polymethacrylate series based on the above structural parameter model. Results from the group contribution method⁹ and connectivity index method² are listed in the same table. Alkyl groups with up to six carbons are included in this table, since data for higher carbon numbers are limited in literature. Due to the fact that the experimental glass transition temperatures of polymers depend on many experimental factors: the rate at which the experiment is performed, the method of measurement, the conditions in which the polymers are synthesized, the crystallinity of the polymers, etc.,²⁴⁻²⁷ experimental T_g values can vary significantly. Therefore, glass transition temperatures from the same source, if possible, are preferred, so as to minimize the possible errors due to the variations in experimental conditions. Reference 24 gave the most T_g values for the four polymers studied here and is thus selected as the major source. These values are also well-supported by many other sources,^{2,21,25,27} from which some missing data from reference 24 are also found (Table I–Table III). It can be seen from the group contribution method that there is a great discrep-

Table II Model Calculation Results for PaS and PO

No. of C	-Alkyl	D	L	D/L	D ² L	Log (D/L)	PaS		PO	
							T_g (Deg C)	T_g After Ref.	T_g (Deg C)	T_g After Ref.
0	H	1.072	1.372	0.781	1.58	-0.107	97	[2, 21, 24, 25]	-20	[25]
1	methyl	2.083	2.316	0.899	10.05	-0.046	101	[2, 21, 24]	-10	[24, 25]
2	ethyl	2.263	3.860	0.586	19.76	-0.232	65	[21]	-24	[24, 25]
3	<i>n</i> -propyl	2.353	5.404	0.435	29.91	-0.361	38	[21]	-40	[24,25]
4	<i>n</i> -butyl	2.406	6.948	0.346	40.23	-0.460	5	[2, 24]	-50	[2, 24, 25]
4	<i>t</i> -butyl	4.455	3.431	1.298	68.10	0.113	126	[2, 21]	64	[25]
5	<i>n</i> -pentyl	2.442	8.492	0.288	50.65	-0.541			-53	[2]
5	<i>t</i> -pentyl	3.539	4.975	0.711	62.29	-0.148			59	[25]
6	<i>n</i> -hexyl	2.468	10.036	0.246	61.13	-0.609	-27	[24]	-64	[24]
7	<i>n</i> -heptyl	2.487	11.580	0.215	71.64	-0.668			-53	[2]
8	<i>n</i> -octyl	2.502	13.124	0.191	82.17	-0.720	-44	[24]		
9	<i>n</i> -nonyl	2.514	14.668	0.171	92.72	-0.766	-53	[24]		
10	<i>n</i> -decyl	2.524	16.212	0.156	103.28	-0.808	-65	[24]		

D and L are in Angstroms.

ancy (170°C) between the experimental glass transition temperature and the calculated one for polystyrene; although, for the other polymers of this series, the deviations are not significant. On the other hand, the discrepancies from the connectivity index method are larger (30°–39°C) for polymers with the higher carbon number substituents, compared to those from the group contribution method and the structural parameter method. The glass transition temperatures from polystyrene to poly(methyl styrene) and to poly(*p-t*-butyl styrene) increase in experimental data; whereas, the connectivity index calculation shows the reverse trend. The deviations from the structural parameter model are generally small and evenly distributed among all polymers within the whole series. The correct order of the change in glass transition temperature of polystyrene, poly(methyl styrene) and poly(*p-t*-butyl styrene) is predicted by the currently proposed method. Similar cases are observed in the polymethacrylate series as shown in the lower part of Table I. Series of polyacrylates and polyolefins are also tested for the calculation, although both the experimental and the calculated data are not as plentiful as those for the alkylated polystyrenes and polymethacrylates. Table II lists the calculated parameters D , L , D/L , D^2L and $\log(D/L)$ for the polystyrene and the polyolefin series that have carbon as their connecting atom. Table III lists those for polymethacrylates and polyacrylates. The volumetric element D^2L is also tabulated as a comparison. The parameters T_{g0} and k are ex-

tracted from fitting the experimental glass transition temperatures against the structural parameter $\log(D/L)$. The results are shown in Table IV Figure 4 and Figure 5. Comparing the fitting of PaS and PO, it is found that all polymers studied in the PaS series are a good fit. The predicted glass transition temperatures show the correct order corresponding to the experimental values (Table I and Table II), regardless of the structures of the substituents, linear or highly branched. The structural parameter $\log(D/L)$ quantitatively balanced the two competing trends of the glass transition temperature effects due to linear lengthening and branching. The D/L value for poly(*p-t*-butyl styrene) at 1.298 is much higher than those for poly(methyl styrene) at 0.899 and polystyrene at 0.781; thus, the glass transition temperature should go in the order of poly(*p-t*-butyl styrene) > poly(methyl styrene) > polystyrene. The volumetric parameter, D^2L , for the linear poly(*p-n*-butyl styrene) at 40 Å³ is smaller than that of the highly branched poly(*p-t*-butyl styrene) at 68 Å³. The limited difference in the volumetric parameter between the two poly(butyl styrenes) does not reflect the huge difference in their glass transition temperatures. Linear poly(*p-n*-butyl styrene) still has a higher D^2L value than poly(*n*-propyl styrene), and thus should have a higher glass transition temperature if volumetric effects are the key factors to be considered in the prediction as found in earlier calculations.⁷ On the other hand, in the case of the polyolefin series, the polymers substituted by lin-

Table III Model Calculation Results for PaMA and PaA

No. of C	-Alkyl	D	L	D/L	D ² *L	Log (D/L)	PaMA	T_g	PaA	T_g
							(Deg C)	After Ref.	(Deg C)	After Ref.
0	H	0.960	1.260	0.762	1.16	-0.118	228	[28]	105	[24]
1	methyl	1.971	2.204	0.894	8.56	-0.049	105	[2, 24]	4	[24]
2	ethyl	2.188	3.748	0.584	17.94	-0.234	65	[24]	-22	[2, 24]
3	<i>n</i> -propyl	2.297	5.292	0.434	27.91	-0.363	34	[2, 24]	-45	[2, 24]
4	<i>n</i> -butyl	2.362	6.836	0.345	38.13	-0.462	20	[2, 24, 28]	-57	[2, 24]
4	<i>t</i> -butyl	4.455	3.431	1.298	68.10	0.113	118	[24, 28]	42	[2]
6	<i>n</i> -hexyl	2.436	9.924	0.245	58.89	-0.610	-5	[2, 24]		
7	<i>n</i> -heptyl	2.459	11.468	0.214	69.36	-0.669			-78	[2, 28]
8	<i>n</i> -octyl	2.477	13.012	0.190	79.86	-0.720	-20	[2, 24]	-65	[2]
9	<i>n</i> -nonyl	2.492	14.556	0.171	90.38	-0.767			-58	[2]
12	-dodecyl	2.522	19.188	0.131	122.03	-0.881	-65	[24]		
18	-octadecyl	2.553	28.452	0.090	185.51	-1.047	-98	[24]		

D and L are in Angstroms.

ear alkyl groups fall on a straight line, while the ones with highly branched sections such as *t*-butyl and *t*-pentyl groups fit in a much higher region in T_g (area A in Figure 4). Obviously, this is due to the close proximity and strong steric interaction of those highly branched groups with the polymer main chains. Since polyolefin has a very small basic unit, it is the backbone unit itself. The curve bounces up in area B, the region where the entanglement of the long side group is offset, and this is excluded from the data fitting process of polyolefins. In Figure 5, data for polymethacrylates and polyacrylates are plotted. Similarly, the middle regions of both plots show good linearity. Region B in the polyacrylate series is again due to the entanglement of the long side group. For both series, the unsubstituted polymers, i.e., poly(methacrylic acid) and poly(acrylic acid), show exceptionally high experimental T_g s. The differences between the experimental and predicted glass transition temperatures is 107°C for poly(acrylic acid) and 144°C for poly(methacrylic acid), as indicated on both plots. The reason for the difference is that in the structural parameter model, only the geometric properties

are considered and other interactions such as H bonding between —OH···O=CO— in the basic units, as in this case, are not considered. However, this difference provides us with an additional angle to view the contribution to the glass transition temperature purely from the H bonding. Realizing that there is the possibility of sizable variation in the glass transition temperature due to experimental conditions,^{24–27} the two differences, 107°C and 144°C, are in good agreement and are a reasonable indication of the H-bonding contribution.

The fitting parameters are listed in Table IV. It is obvious from eq. (6), that T_{g0} determines the major region of glass transition temperature and is believed to depend on the basic unit of each polymer, i.e., the size and the rigidity of the basic unit. The phenyl group is one of the most rigid groups, as is the α -methyl group on the backbone.²⁵ Those rigid and bulky groups make it difficult for the backbone to move cooperatively in a large scale and thus, a higher T_{g0} value results. Obviously, the —COO— group exerts additional difficulty for the polymer chain of polyacrylates to move. This is seen from its slightly higher T_{g0}

Table IV Correlation Parameters for PaS, PO, PaMA and PaA

	PaS	PaMA	PaA	PO
T_{g0} (deg C)	110.76	106.71	16.36	-6.73
k (deg C)	216.37	189.60	152.75	90.79
Fit SD	6.14	7.12	7.16	2.91
Correlation factor r^2	0.993	0.992	0.979	0.982

value when comparing the polyacrylate and the polyolefin series. The constant k reflects the dependency of the glass transition temperature on the parameters of the substituents. The k values show similar trends for all the series, with the polyolefin series having the lowest value. This is an indication that the addition of an alkyl side group has the least effect for polyolefins. This is reasonable due to the same chemical and structural nature of both the backbones and the side groups in polyolefins.

CONCLUSIONS

The structural parameter method, based on the flexible features of alkyl substituent groups,

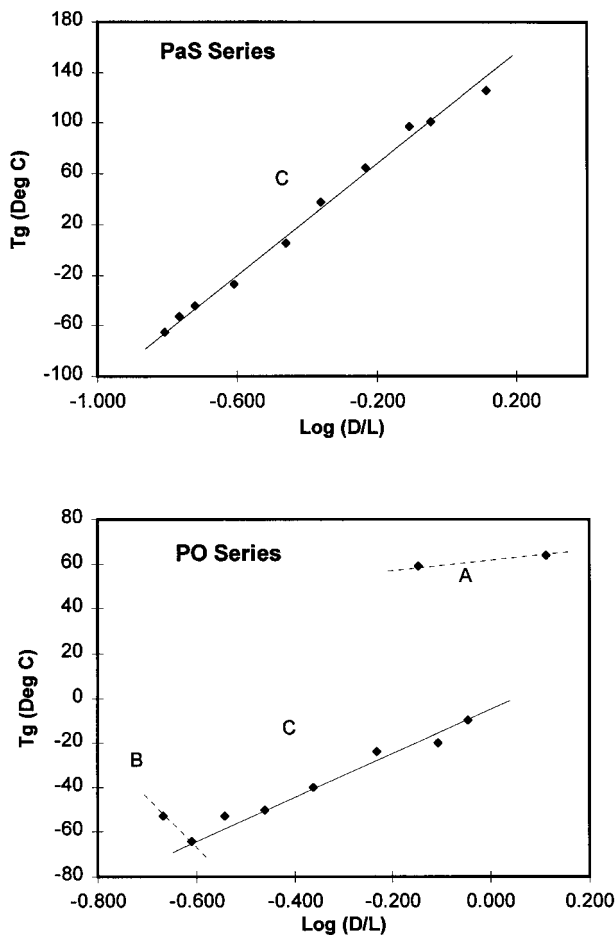


Figure 4 Data fitting plots for poly(alkyl styrene) (PaS) series and polyolefin (PO) series. Region A shows the strong steric interaction between the highly branched section and the main chain. Region B reveals the entanglement of long side chains. Region C represents the linear range that is utilized for the data fitting.

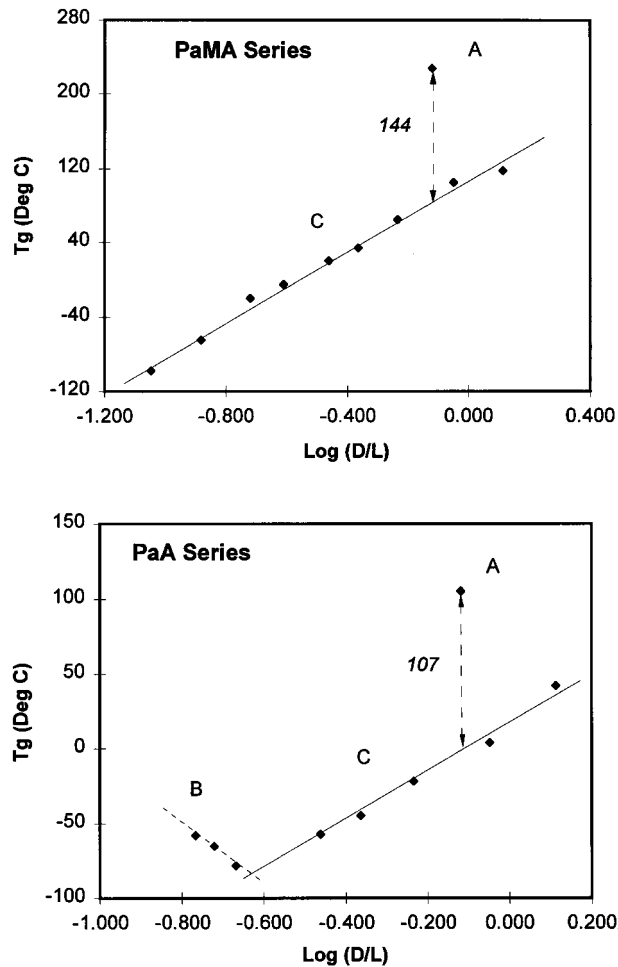


Figure 5 Data fitting plots for polymethacrylate (PaMA) series and polyacrylate (PaA) series. Point A on both plots represents the unsubstituted polymers, poly(methyl methacrylic acid) and poly(acrylic acid). Region B reveals the entanglement of long side chains. Region C represents the linear fitting range that is utilized for the data fitting. The differences between the experimental (point A) and the calculated values are indicated on the plots, which reveal the contribution of H-bonding to the glass transition temperatures.

shows a consistent prediction of the glass transition temperature for both the linear and highly branched polystyrenes in the authors' research. The same model is also well-suited for three other polymer systems: polyolefins, polymethacrylates and polyacrylates. The two basic competing influences of the structural modification of polymers on their glass transition temperatures are linear lengthening to decrease the T_g resulting from the plasticizing effect, versus branching to increase the T_g due to the steric effect. The competing influences are well-balanced by the parameter log

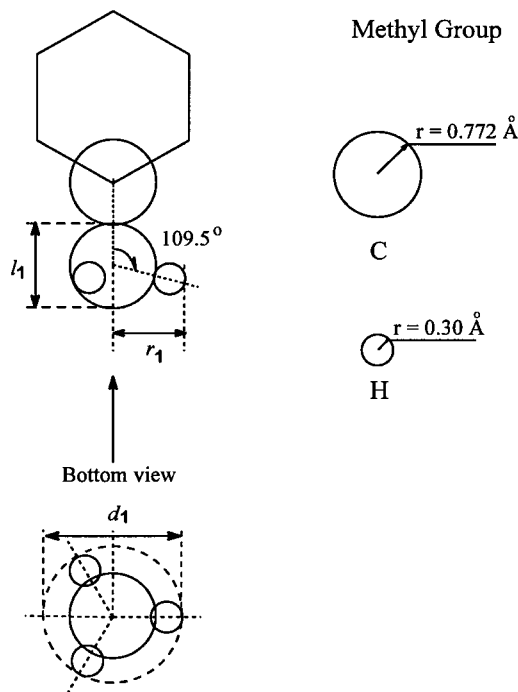


Figure A.1 Calculation diagram for the sections with primary, secondary and tertiary carbons, where there is at least one terminal H atom. The methyl group is shown here.

(D/L). This is shown by the correct prediction that *t*-butylated polymers should have much higher glass transition temperatures, followed by the methylated polymers, as compared to the unsubstituted polymers. It has been shown that the structural parameter $\log (D/L)$ quantitatively correlates structural aspects with the glass transition temperature of various systems where various alkylations occur. The current model permits the extraction of the contribution of the hydrogen bonding to glass transition temperature in polymethacrylates and polyacrylates. The size and rigidity of the basic units of the four polymers studied are reflected in the data parameters, T_{g0} and k . The highest values for both are given by the polystyrene series, due to the bulky and rigid phenyl group present. Polyolefins have the smallest values, due to their small and flexible $-C-C-$ structures.

APPENDIX: THE CALCULATION OF GEOMETRIC PARAMETERS OF ALKYL SECTIONS

The bond radii for single bonded H, C and O used in the calculation are from reference 28. For H,

the bond radius is 0.30 Å; for C, 0.772 Å; and for O, 0.66 Å. The two dimensions for H (not shown), d and l are easy to determine, since $d = l = 0.30$ Å. Figure A.1 shows the geometry of the common section for the primary carbon as in the $-CH_3$ section, the secondary carbon as in the $-CH_2-$ section, and the tertiary carbon as in the $-CH=$ section. All three types of carbon are bonded with at least one hydrogen atom as a terminal atom which can reach a radius of r_1 . The tetrahedral bond angle (109.5°) is assumed. As can be seen from the projection, the freely rotating radius of the hydrogen atom(s) is

$$r_1 = (0.772 + 2 \times 0.30) \cdot \cos (109.5^\circ - 90^\circ) = 1.293 \text{ \AA} \quad (\text{A.1})$$

Thus the diameter is

$$d_1 = 2r_1 = 2.586 \text{ \AA} \quad (\text{A.2})$$

Due to the relatively small size of hydrogen atoms compared to carbon atoms, hydrogen does not contribute to the length, l_1 , of this calculation as can be seen visually from Figure A.1 and also from the 3-D ball modeling in Figure A.2. Calculation

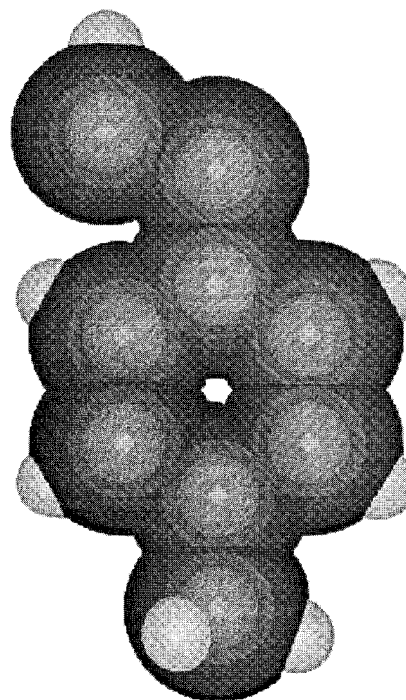


Figure A.2 3-D ball modeling plot of poly(*p*-methyl styrene). As can be seen, the H atoms do not contribute to the section length, l , since they sit above the lowest point of the carbon to which they are attached.

shows that this hydrogen is 0.114 Å above the lowest point of carbon to which it is bonded. Therefore, the length of the section is determined to be,

$$l_1 = 2 \times 0.772 = 1.544 \text{ \AA} \quad (9)$$

The terminal hydrogen atoms in highly branched alkyl groups, such as *t*-butyl and *t*-pentyl groups, extend beyond the central quaternary carbon. Figure A.3 shows the quaternary structure where the maximal geometry of the structure can be achieved for a *t*-butyl group. Figure A.4 shows the 3-D ball modeling that corresponds to this structure. The maximum section radius r_3 and diameter d_3 as shown by the projection on the bottom in Figure A.3 are given as follows:

$$\begin{aligned} r_2 &= 2 \times 0.772 \cos(109.5^\circ - 90^\circ) + 0.772 \\ &= 2.227 \text{ \AA} \quad (10) \end{aligned}$$

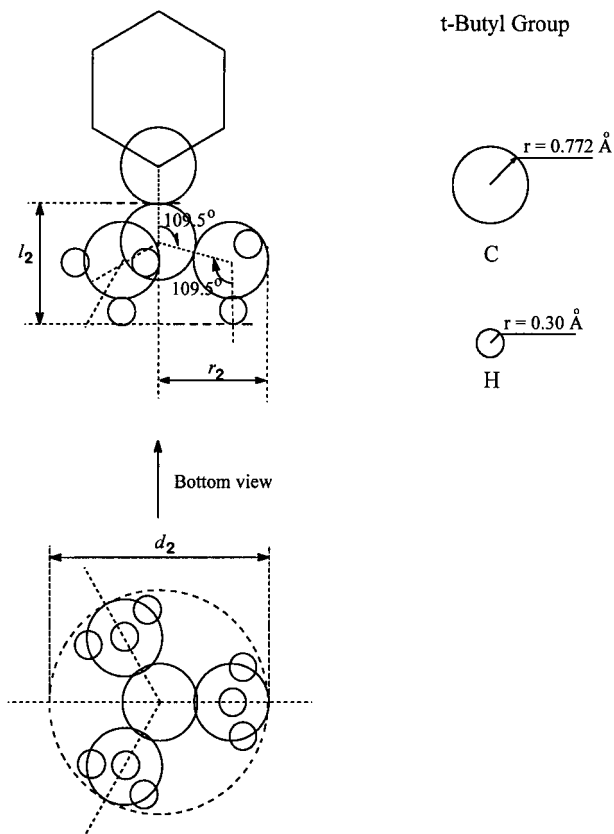


Figure A.3 Calculation diagram for the section with highly branched, quaternary carbon. The *t*-butyl group is shown here.

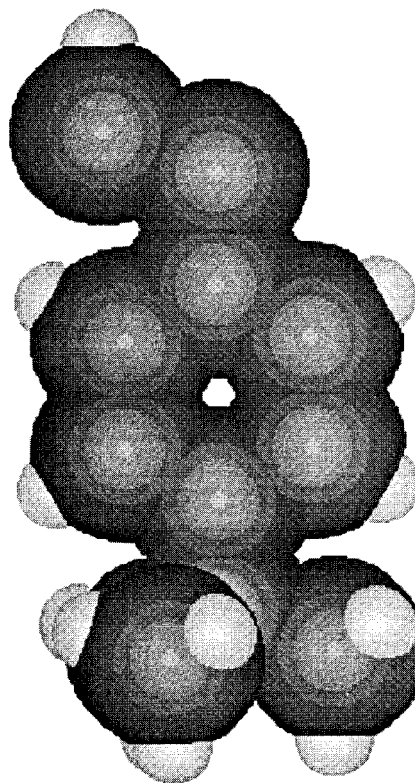


Figure A.4 3-D ball modeling plot of poly(*p*-*t*-butyl styrene). Terminal hydrogens extend beyond the central quaternary C. The *t*-butyl group forms an umbrella that contains the connecting C atom.

$$d_2 = 2r_2 = 4.454 \text{ \AA} \quad (11)$$

The maximum section length is

$$\begin{aligned} l_2 &= 0.772 + 2 \times 0.772 \sin(109.5^\circ - 90^\circ) \\ &\quad + 0.772 + 2 \times 0.300 = 2.659 \text{ \AA} \quad (12) \end{aligned}$$

REFERENCES

1. *Computational Modeling of Polymers*, J. Bicerano, Ed., Marcel Dekker, New York, 1992, Chap. 1, pp. 77–83.
2. J. Bicerano, in *Prediction of Polymer Properties*, D. Hugdin, Ed., Marcel Dekker, New York, 1993, Chap. 6.
3. D. Potter, *Group Interaction Modeling of Polymer Properties*, Marcel Dekker, New York, 1995, Part 3.
4. B. Frick and B. Richter, *Science*, **267**, 1939 (1995).
5. P. S. Subramanian and K. J. Chou, *Trends in Polymer*, **3**, 324 (1995).
6. R. A. Hayes, *J. Appl. Polym. Sci.*, **5**, 318 (1961).

7. K. Marcincin and A. Romanov, *Polymer*, **16**, 173 and 177 (1975).
8. U. T. Kreibich and H. Batzer, *Angew. Makromol. Chem.*, **83**, 157 (1979).
9. D. W. van Krevelen and P. J. Hoftyzer, *Properties of Polymers*, Elsevier, Amsterdam, 1976, Chap. 6.
10. A. C. Puleo, V. Muruganandam, and D. R. Paul, *J. Polym. Sci., Part B, Polym. Phys.*, **27**, 2385 (1989).
11. P. I. Vincent, *Polymer*, **13**, 558 (1972).
12. S. M. Aharoni, *J. Appl. Polym. Sci.*, **20**, 2863 (1976).
13. B. F. Boyer and R. L. Miller, *Macromolecules*, **10**, 1167 (1977).
14. B. F. Boyer and R. L. Miller, *J. Polym. Sci., Polym. Phys. Ed.*, **16**, 371 (1978).
15. T. B. He, *J. Appl. Polym. Sci.*, **30**, 4319 (1985).
16. V. P. Privalko, *Macromolecules*, **6**, 111 (1973).
17. K. K. Chee, *J. Appl. Polym. Sci.*, **43**, 1205 (1991).
18. A. J. Hopfinger, M. G. Koehler, R. A. Pearlstein, and S. K. Tripathy, *J. Polym. Sci.: Part. B: Polym. Phys.*, **26**, 2007 (1988).
19. J. Han, R. H. Gee, and R. H. Boyd, *Macromolecules*, **27**, 7781 (1994).
20. D. R. Wiff, M. S. Altieri, and I. J. Goldfarb, *J. Polym. Sci., Polym. Phys. Ed.*, **23**, 1165 (1985).
21. H. Gao and J. P. Harmon, *Thermochimica Acta*, to appear.
22. J. P. Harmon and H. Gao, in *Proceedings of the 24th North American Thermal Analysis Society Conference*, 1995, p. 325.
23. H. Gao and J. P. Harmon, *Abstracts of Papers*, American Chemical Society Florida Sections 1995 Joint Annual Meeting, Orlando, FL, 1995, SLVIII, p. 31.
24. J. E. Mark, A. Eisenberg, W. W. Graessley, L. Mandelkern, E. T. Samulski, J. L. Koenig, and G. D. Wignall, in *Physical Properties of Polymers*, A. Rouhi, Ed., 2nd ed., American Chemical Society, Washington, DC, 1993, p. 77.
25. M. P. Stevens, *Polymer Chemistry*, 2nd ed., Oxford University, New York, 1990, p. 80.
26. J. A. Brydson in *Polymer Science*, A. D. Jenkins, Ed., North-Holland, Amsterdam, 1972, Chap. 3.
27. *Polymer Handbook*, J. Brandrup and E. H. Immergut, Eds., Wiley, New York, 1989, Chap. VI.
28. I. N. Levine, in *Physical Chemistry*, K. Misler and S. Tenney, Eds., McGraw-Hill, New York, 1988, p. 653.